Elsevier Editorial System(tm) for Biosensors and Bioelectronics

Manuscript Draft

Manuscript Number:

Title: Reduced Graphene-Oxide Transducers for Biosensing Applications Beyond the Debye-Screening Limit

Article Type: VSI:Biosensors2018

Section/Category: The others

Keywords: reduced graphene-oxide thin-films; in-line electrochemical impedance spectroscopy; aptasensor; Debye-screening limitation

Corresponding Author: Professor Sven Ingebrandt, Prof. Dr.

Corresponding Author's Institution: University of Applied Sciences Kaiserslautern

First Author: Xiaoling Lu

Order of Authors: Xiaoling Lu; Anna Moidek; Walid Munief; Pawan Jolly, PhD; Vivek Pachauri, Dr.; Xianping Chen, Prof. Dr.; Pedro Estrela, Prof. Dr.; Sven Ingebrandt, Prof. Dr.

Reduced Graphene-Oxide Transducers for Biosensing Applications Beyond the Debye-Screening Limit

Xiaoling Lu[1,2], Anna Moidek[3], Walid Munief[2], Pawan Jolly[3,4], Vivek Pachauri[1,2], Xianping Chen[5], Pedro Estrela[3], Sven Ingebrandt[1,2]*

[1] Institute of Materials in Electrical Engineering 1, RWTH Aachen University, Aachen, Germany

[2] Department of Informatics and Microsystem Technology, University of Applied Sciences Kaiserslautern, Zweibrücken, Germany

[3] Department of Electronic and Electrical Engineering, University of Bath, Bath, United Kingdom.

[4] Present address: Wyss Institute for Biologically Inspired Engineering at Harvard University, Harvard Medical School, Boston, USA

[5] Key Laboratory of Optoelectronic Technology & Systems, Education Ministry of China and College of Optoelectronic Engineering, Chongqing University, Chongqing, China

*corresponding author: ingebrandt@iwe1.rwth-aachen.de

Abstract

In the field of label-free biosensing, various transducer materials and strategies are under investigation to overcome the Debye-screening limitation of biomolecule charges, which is a main limiting factor to detect clinically relevant biomarkers in physiological matrices. We demonstrate an in-line, impedimetric aptasensor with reduced graphene-oxide (rGO) thin films as transducers to detect prostate specific antigens (PSA). Unlike classical electrochemical impedance spectroscopy (EIS), this direct, label-free and fully-electronic biosensor approach does not need any redox markers. PSA dose-response experiments were done in phosphate buffer solution with physiological concentration with a theoretical Debye screening length of 0.76 nm. As specific capture molecules, short anti-PSA aptamers ensured a close binding of the target molecules to the transducer surfaces. Results showed a limit of detection smaller than 33 pM of PSA and a pronounced detection scale from 33 pM to 330 nM fully covering the clinically relevant range of PSA (115 - 290 pM). This promising performance is attributed to the bipolar electronic transport behavior of our ultra-thin rGO layers similar to pristine graphene. The attachment of target biomolecules to the films changes the surface potential resulting in a resistance change inside the rGO thin films. Such an in-line EIS with rGO thin films opens promising prospects for biosensing beyond the Debye-screening limitation, which is a major challenge for conventional semiconductor field-effect devices towards clinical applications.

Index Terms

reduced graphene-oxide thin-films, in-line electrochemical impedance spectroscopy, aptasensor, Debye-screening limitation

1. Introduction

Electrochemical impedance spectroscopy (EIS) (Orazem and Tribollet, 2011),(Lisdat and Schafer, 2008),(Barsoukov and Macdonald, 2005),(Macdonald, 2005),(Macdonald, 1990) is widely used as a promising sensitive, selective and label-free biosensing principle in solutions to analyze biorecognition events on their sensor surfaces. The technique extracts the complex impedance of a system under test by applying an alternating voltage perturbation of small amplitude (generally mV) in a certain frequency range and measuring the current response. Conventional EIS can be classified into faradaic and non-faradaic modes. Faradaic EIS measurements are usually done in the presence of redox molecules in the test solution and the amount in redox current varies by the electronic property of the working electrode. When biomolecules are binding to these electrodes, their accessible surface gets smaller and hence the redox current is reduced. Current decrease can then be related to the receptor-analyte binding at the surface and concentrations of analyte molecules can be measured. The total faradaic current also strongly relies on the electronic properties of the biomolecules, since some of the biomolecules can be redox-active, but most of the biomolecules act as insulating layer.

For the non-faradaic EIS, the impedance measurement is carried out in absence of redox molecules to reveal the biorecognition event (Bart et al., 2005). A classical device configuration are interdigitated electrodes (IDEs), which are described as capacitive biosensors (Berdat et al., 2008),(Berdat et al., 2006),(Yang et al., 2004). They are known to exhibit a high sensitivity due to the confinement of the local electrical field closely inside the micrometer-size IDEs structures. In both faradaic and non-faradaic

EIS, conventional impedance measurements are detecting impedance changes of the biosystem between counter and working electrode by passing current through the buffer solution on top of them. Advanced transducer layers can be additionally applied in between the IDE finger electrodes and the biorecognition layer to amplify the output signals and to enhance the sensitivity of the sensors. In many cases, this improvement stems from improved immobilization density of the bio-recognition molecules on the EIS biosensor surface.

In recent years in the field of biosensor and bioelectronics, chemically exfoliated graphene oxide (GO) and reduced graphene oxide (rGO) attracted plenty of attention due to its similarity to pristine graphene. Graphene (Novoselov et al., 2004),(Castro Neto et al., 2009),(Geim and Novoselov, 2007),(Novoselov et al., 2012),(Kahng et al., 2012),(De and Coleman, 2010),(Baringhaus et al., 2014),(Huang et al., 2011) is an atomic 2D material and consists of a carbon hexagonal lattice that possesses high carrier mobility, excellent mechanical properties, high thermal stability and good biocompatibility. GO (Dreyer et al., 2010),(Eda and Chhowalla, 2010) and rGO (Bagri et al., 2010),(Gómez-Navarro, 2007),(Pei and Cheng, 2012) thin-films not only preserve this carbon lattice alike graphene to maintain the above-mentioned, promising properties within nanoscale, but also own various functional oxygen groups on their carbon basal plane. This is beneficial for chemical attachment of capture molecules to the thin films. Therefore, these two materials are intensively exploited as alternatives to overcome the dilemma that graphene is facing towards its wafer-scale fabrication and process integration (Suk et al., 2011),(Liang et al., 2011) such as robust, cost-effective biosensor device preparation, further-advanced surface functionalization and chemical

functionalization with receptor biomolecules. In most of the cases, rGO thin-films (Bonanni et al., 2012b)'(Bonanni et al., 2012a) are utilized as transducer layers in conventional, faradaic EIS to enhance the sensing area by various functional oxygen groups on its carbon basal plane.

In the present study, an in-line EIS biosensor platform was developed with rGO thin-films as transducer layers on top of IDEs (Zaretsky et al., 1988)'(Igreja and Dias, 2004), while the impedance was measured along the rGO thin-film. This biosensor transducer principle is working in a label-free mode without the use of any redox markers. Since in this configuration the IDE electrodes are bridged by a conductive material, already at low frequencies (1 Hz) significant changes in the impedance values upon biomolecule binding are visible. The promising semi-metal properties of rGO with a strong reaction to surface potential changes at the solid-liquid interface were advantageous for biosensing. In addition a short, 32 base pair anti-PSA aptamer sequence as ultra-thin biorecognition layer (Jolly et al., 2015)'(Formisano et al., 2015) enabled the detection of PSA in physiological buffer solutions. The electronic signal confinement at the IDE sensor spots for both rGO thin films and IDEs demonstrate a precedential biosensing capability beyond the typical Debye-screening limit in aqueous solutions.

2. Materials and Methods

2.1. Chemicals and Reagents

Amine-terminated, PSA-specific DNA aptamer (5'-NH2-(CH2)6 –TTTT TAAT TAAA GCTC GCCA TCAA ATAG CTTT-3') and (3-Aminopropyl) triethoxysilane (APTES) were purchased from Sigma Aldrich, Germany. PSA was obtained from Merck Chemicals Ltd.

(Beeston, UK). For the electronic assays, phosphate buffer solution (PB) with pH 7.4 and 10 mM concentration was prepared from monohydrate phosphate and dinatrium hydrogen phosphate salts. Other chemicals for biofunctionalization and biosensing experiments as mentioned in the following were purchased from Sigma Aldrich and used without further purification.

2.2. Preparation of GO flakes

GO flakes were chemically exfoliated by the improved Hummers' method with additional purification and cleaning of GO in further steps. 4g graphite powder (Alfa Aeser, natural, -325 mesh, 99.8%) as base material was fully oxidized and exfoliated in a reflux condenser with a mixture of H_2SO_4 and H_3PO_4 for 24 hours. To restrict the destructive power to the carbon lattice but not heavily slow down the exfoliation speed, the reaction temperature was stabilized by a cooling water flow system at a mild temperature of 20° C. Subsequent to the reaction, the mixture was quenched with 400 ml ice water mixed with 4 ml H_2O_2. The obtained GO solution was filtered through a stainless steel sieve (200 µm, Spoerl OHG) lined with a polyester fiber. It was essential to eliminate all ionic products Mn^{2+}, SO_4^{2-}, PO_4^{3-} and K^+ out of the dispersion, which was realized with a dialysis membrane (25.4 mm, Th. Geyer GmbH & Co.KG). Dialysis was repeated two times to avoid ion inclusions after drying the dispersed GO. Afterwards, the dialyzed GO dispersion was mixed with DI water and three times centrifuged at 4500 rpm for 45 min until the last supernatant reached at pH value of 2.0. Furthermore, the GO mass was mixed with 200 ml HCl and then centrifuged at 4500 rpm for 45 min, following by the same step two times in C_2H_5OH (98 %). Each centrifuge step was followed by GO solution filtering in the polyester fiber sieve. The obtained residue was coagulated with

150 ml diethyl ether and filtered through the sieve lined with a PTFE filter with mesh size of 0.45 µm. The filtered graphene oxide was evacuated for 48 h in the desiccator to dry it. The lateral sizes of the resulting flakes ranged from 300 nm to 20 µm due to aggregation of the material in the sieve. To obtain lateral mono- and multi-layer GO flakes, the dispersion was centrifuged again for two times at 1000 rpm until a final pH value of 2.9. GO was water soluble and could be applied in the next steps as spin-coating solution to form ultra-thin GO films.

2.3. Fabrication of GO thin films and devices

In present study, the GO thin films were prepared on 4-inch wafers in a routine clean room process. Glass or SiO_2/Si wafers were thoroughly cleaned with freshly prepared Caro's acid (H_2O_2 (30 w %), azeotropic H_2SO_4 (98 w %) ratio 1:3, T = 120 °C, t = 20 min). Afterwards, the wafers were activated by O_2 plasma (t = 5 min, 230 W) and functionalized by APTES in a gas-phase silanization process. The Au coated surfaces were preferably positioned at an angle of about 85 ℃ with respect to the outlet valve of the desiccator to provide a maximum contact area between the substrate and the silane-saturated gas stream. Then, the pressure inside of the desiccator was gradually reduced to 130 mbar such that a continuous gas flow of the silane over the substrate was ensured. The reaction time was 2 h. In this process, the surface -OH groups replace the O-CH_2-CH_3 ethoxy-group by a SN_2 reaction forming the corresponding 3-Aminopropylsiloxane APS on the wafer surface (Schmitt, 2014)(Schmitt et al., 2015). After the silane coating, the wafer was washed with ethanol. The -NH_2 groups on the other end of the APS layer, which are accessible on the surfaces can covalently bind

GO flakes by reacting with their -COOH groups. 5 mL GO solution *pH* = 2.9 prepared was applied and spin-coated onto the wafer surface. The process details can be found in a previous publication (Lu et al., 2018).

2.4. Thermal reduction of GO devices

The prepared GO devices were placed inside a vacuum oven (VT5042 EKP, Heraeus, Germany) at 350 °C for 10 h to remove the oxygen functional groups and to reduce the material gradually. Afterwards, to generate ohmic contacts between the thin films and the Au electrodes underneath, the devices were rapidly annealed in a high temperature oven (DS-3900-PC-150, INOTHERM, Germany) at 600 °C for 20 s in ambient air. GO flakes inside a film are then reduced to rGO and the network of flakes forms a quilted layer with bipolar electronic transport properties similar to pristine graphene but with much smaller carrier mobilities.

2.5. rGO thin-film based in-line EIS device

In the present study, rGO-IDEs devices were used. They were fabricated in the clean room at Zweibrücken campus of the University of Applied Sciences Kaiserslautern, Germany. IDEs were primarily prepared on 4−inch glass wafers by standard photolithography (MA/BA 6, Süss, Germany), metal evaporation (BAK500, Oerlikon Balzers, Liechtenstein) and lift-off processes. The electrode material was a bilayer stack: top layer was 270 nm Au and bottom layer was 30 nm Ti, which acted as an adhesion layer. Overall, we fabricated 72 chips in parallel on the 4-inch wafers. Each chip was 7x7 mm^2 in size and consisted of a 4x4 array with in total 16 individual drains sharing a common source-electrode. The resistance and capacitance of each drain electrode was

designed to be equal for accurate comparison of measurement results between the 16 channels. The width and length of a single drain electrode was 5 µm and 100 µm, respectively, while the separation distance of the neighboring electrodes was 5 µm. In the case of 10 electrode fingers, the effective channel length and width of IDEs were 5 µm and 1000 µm, respectively. The GO thin film was formed on top of already prepared IDEs using spin-coating. This procedure forms ultra-thin but uniform GO films in the range of 1.5 – 2 nm per spin coating step. In total six spin-coating steps were applied for the devices used here in order to ensure complete films without defects. For patterning of the GO thin films, we applied standard photolithography. Afterwards, the films were protected by photoresist and the unprotected rest was completely etched away by O_2 reactive ion etching (SI 591 M, SENTECH, Germany).

2.6. Biofunctionalization of rGO thin-film based in-line EIS biosensor

In present study, the detailed biosensor preparation procedure with aptamers as receptor biomolecules for the PSA dose-response experiments in 10 mM PB solution was as following: 80mM N-(3-Dimethylaminopropyl)-N′-ethylcarbodiimide hydrochloride (EDC) mixed with 20mM N-Hydroxysuccinimide (NHS) in milliQ water (resistivity 18.2 MΩ·cm) was prepared to activate the -COOH groups on the surface of the rGO thin films for a covalent immobilization of the amino-terminated aptamers. 100µL of EDC/NHS solution was applied on the rGO thin films for 30 mins at room temperature. The amino-terminated aptamers were treated as following to gain an optimal position to capture the PSA molecules: The microcentrifuge tube, which contained 10 µL of 100 µM amino-terminated aptamers was taken out of the freezer and laid in the room temperature for approximate10 mins to defreeze it. Fast spinning was applied for 5 seconds to collect the residual droplets on the

tube's sidewall. Then the microcentrifuge tube was immersed at half of is height into a flask containing 90 °C hot milliQ water. After the temperature was cooled down to room temperature, the microcentrifuge tube was taken out and centrifuged for 5 seconds. The 100 µM amino-terminated aptamers were diluted to 2 µM by 10 mM PB with a final pH = 7.4. 100 µL of 2 µM aptamer solution was applied on the rGO thin films for 30 mins at room temperature immediately after their EDC/NHS activation. The chips were incubated in 2 µM aptamer solution overnight at 4°C. Afterwards, the chips were cleaned for 10 times by flowing PB. A blocking solution of 1 mM ethanolamine (pH = 8.5) was prepared by diluting with PB and applied on the rGO thin films for 30 mins. This blocking procedure saturated the remaining -COOH groups of rGO and suppressed non-specific binding of target biomolecules to the surfaces. The different concentrations of PSA for the calibration curve were prepared by diluting 100 µM stock solution in 10 mM PB solution. The dose-response measurements started by incubating the chips in 100 µL PSA with a concentration of 33 fM for 30 mins. After each step, the chips were cleaned for 10 times by 10 mM PB and recorded in the in-line EIS configuration by an impedance analyzer (Ivium COMPACTSTAT.e, Ivium Techologies, Netherland). The same process was repeated by stepwise adding higher PSA concentrations onto the rGO biosensor surfaces as following: 330 fM, 3.3 pM, 33 pM, 330 pM, 3.3 nM, 33 nM and 330 nM.

2.7. Control experiments with Human Serum Albumin (HSA)

To check the specificity of the rGO biosensors, the sensor surface was prepared similarly to the protocol described under paragraph 2.6 but without the aptamer immobilization. A highly concentrated stock solution of 100 µM human serum albumin (HAS) was prepared in 10 mM PB (pH~7.4) and subsequently filtered by a filter with

pore size of 0.2 µm. The test solution of 1 µM HSA was prepared by diluting the 100 µM stock solution in 10 mM PB (pH~7.4). In the control experiments, this non-specific solution was applied similarly to the PSA solutions.

2.8. Fluidics setup

A fluidics setup was printed by a 3D printer (Objet350 Connex, Stratays Ltd., Israel). It contained two top and bottom parts. The top part had a container in its center and a sealing rubber ring at the side. The IDE rGO sensor chips were clamped between these two parts, while the rGO arrays were exposed to the liquid. Details of this measurement cell were described earlier (Lanche et al., 2014). All of the surface functionalization and sensor measurements were carried out within this fluidic cell.

2.9. Measurement setup

In the present study, an in-line EIS configuration for the IDE rGO devices was used. The EIS measurements were carried out with the two arms of the IDEs acting as working electrode (WE) and counter electrode (CE), while an electrochemical Ag/AgCl electrode (DRIREF-2SH, WPI, Germany) served as reference electrode (RE). This configuration is denoted as in-line EIS in the following. The electronic performance of the IDE rGO sensors were compared in 10 mM PB buffer solution under the following conditions: the DC offset potential and AC signals were applied to the WE against a constant potential at the RE, the standard potential of which is 0.21 mV in 3 M KCl at room temperature. Before the electronic measurements, an equilibration time of 30 s was allowed after applying the DC bias voltage. The DC potential offset was 50 mV while the AC stimulation voltage was 10 mV in amplitudes. The frequency range was scanned from 100 kHz to 0.1 Hz. The alternating current output I_{out} (t) flowing from the WE to the CE was then measured by the

impedance spectrometer. The 10 mM PB test solution was prepared by dissolving PB tablets in highly pure milliQ water (resistivity 18.2 MΩ·cm) with a final pH value of 7.4.

3. Results

We established an aptasensor platform with rGO thin films as transducer layers on top of interdigitated electrodes to detect PSA. The biosensor devices were measured with a configuration of in-line EIS in 10 mM PB buffer solution (ionic strength 162 mM), which determines a Debye screening length of charges in the solution of 0.76 nm. By performing the dose-response biosensing experiments, we found that the rGO based aptasensor exhibit precedential biosensing capability beyond the Debye-screening limit, as well as a wide sensing range covering the clinically relevant concentration range of PSA.

3.1. rGO-IDEs device

Our devices consist of ultra-thin rGO films, which are composed of small GO flakes and are structured on top of 16-channel IDEs arrays on glass wafers. Graphene oxide flakes were chemically exfoliated by an improved Hummers' method (compared materials and methods section) and spin-coated on top of APTES-functionalized wafer surfaces with pre-fabricated IDEs arrays. The spin-coating procedure is forming uniform thin films, which were subsequently patterned into microstructures by standard photolithography and O_2 plasma etching processes. A scanning electron microscopy (SEM) image of an exemplary rGO IDEs electrode structure is shown in **Fig. 1A**. The thickness of the GO patterns were measured by atomic force microscopy (AFM) and were 8 nm thickness, as shown in **Fig. 1B**.

3.2. Electronic performance of the rGO based in-line EIS

In the present study, the in-line EIS measurements were carried out with a three electrodes potentiostat setup, as schematically shown in **Fig. 2A**. The two arms of the IDE structures and the Ag/AgCl electrode served as working (WE), counter (CE) and reference (RE) electrodes, respectively. A sinusoidal voltage V_{in} (t) input was applied to the WE, which changes its potential relative to the fixed potential of the RE. The alternating current I_{out} (t) output which flowed from WE to CE was recorded. The quotient of V_{in} (t) / I_{out} (t) is marked as impedance Z of the IDE sensor. In our measurements, the input V_{in} (t) was of 10 mV amplitude in a frequency range from 1Hz to 100kHz and a DC bias voltage of 50 mV. In 10 mM PB solution, a typical Bode plot of the rGO in-line EIS in shown in **Fig. 2B**. In the quilted rGO thin film the overlapping regions of neighboring rGO flakes bridge the path and meanwhile constrain the direction of carriers' transportation inside the thin film. An electronically equivalent circuit of the rGO thin film can be composed as a resistor R_{rGO}, representing the current transport inside the rGO flakes, in parallel with a capacitor C_{rGO}, representing the capacitive flake-to-flake transport. The current from on side of the IDE to the other side could then pass through the electrochemical double layers (EDLs) at the electrode contacts in series with the ohmic solution R_{sol} or in parallel to this through the rGO thin film from WE to CE. The EDL is not an ideal capacitor, which can be represented by a CPE for both WE and CE. By considering the resistance and capacitance of the rGO thin films into pre-developed circuits for bare IDE biosensors (Berdat et al., 2008), an equivalent circuit for our rGO in-line EIS can be extracted as indicated in **Fig. 2C**.

3.3. PSA biosensing by rGO based in-line EIS

In this study, the aptamer sequence used for PSA detection (Jolly et al., 2015)(Formisano et al., 2015) was TTT TTA ATT AAA GCT CGC CAT CAA ATA GCT TT from 5' to 3'. The 5’ end was modified by a 6-carbon chain as a spacer and terminated with an amino group for covalent tethering to the sensor surface. 10 mM ethanolamine was used as blocking agent to saturate the free-standing -COOH groups on the biosensor surface. The schematic of the biosensor surface preparation flow is shown in **Fig. 3A**. Typically, the 10 mM PB solution has an ionic strength of 162 mM, which results in a Debye length 0.76 nm. The aptamer size is approximately 3-5 nm for a fully stretched molecule. Upon folding into the 3D aptamer structure this size should be smaller. The target molecule PSA is of 33 kDa size and its typical diameter is approximately 4.5 nm. Based on the Debye screening effect, the depictive schematic with folded aptamers as receptor biomolecules to detect PSA on rGO thin film is shown in **Fig. 3B**

To reveal the biosensing capability of the rGO IDE aptasensor for detecting PSA impedance signals for the dose-response experiments were addressed in the full frequency range from 1Hz to 100 kHz, as shown in the Bode plot in **Fig. 4A**. A close-up of the impedance amplitude at the low frequency range 1 Hz to 5 Hz is given in **Fig. 4B**. The biosensing capability to cover the PSA clinically relevant concentration range is demonstrated by recording a calibration curve of impedance amplitudes at a small frequency $f = 1\ \mathrm{Hz}$, as shown in **Fig. 4C**. Five channels are summarized and small error bars indicate a very reproducible sensor response. A control experiment with a high concentration of HAS showed no response (compare individual data point in **Fig 4C**), demonstrating a highly specific detection of PSA.

4. Discussion

Globally, the prostate cancer is one of the leading cause of the cancer-related death in men (Baade et al., 2009). As a most common representative biomarker, PSA is used to address the presence of prostate cancer and identify the relapse after receiving the cancer treatment (Antenor et al., 2005). To detect PSA, plenty of efforts are dedicated to exploit the biosensing capability of various nano-/micro- devices to achieve a perfect biosensor: highly selective, robust, reliable, cost-effective, disposable, environmentally friendly, portable towards point of care usage, with an optimized response to cover the clinically relevant concentration range of PSA. However, the currently available label-free miniaturized biosensors for quantitative detection of PSA severely encounter the Debye-screening limitation in physiological matrices.

In this study, we developed an aptasensor with rGO thin films as transducer layers in an in-line EIS device configuration and we tested this biosensor platform to detect PSA in similar ionic strength as physiological matrices. The PSA dose-repose experiments demonstrated a biosensing capability beyond the Debye screening limitation. This result was additionally corroborated by the dose-response experiments of I-V dual sweep, which provides an additional proof to reveal the predominated sensing mechanism (supporting information **S3**).

All rGO-IDE devices used in this study were prepared on a 4-inch wafer from the same fabrication bench. The detailed chemical exfoliation procedure to generate GO aqueous solution, various characterizations of the GO material, the preparation flow for GO thin-films, and rGO thin film and device fabrication were detailed in our previous publication (Lu et al., 2018). In the present work, the GO aqueous solution was spin-coated on

IDEs structure 8 times to form GO thin-films which are complete without pinholes and which are topographically uniform. After thermal reduction in vacuum oven at 350°C for 10 hours and subsequent fast annealing in a high temperature oven at 600 °C for 20 seconds in the ambient, the GO thin-films was transformed into rGO thin-film. The rGO thin-films were patterned by standard photolithography and O_2 reactive ion etching for SEM and AFM characterizations (Fig. 1a-1b), which indicates that the thickness of rGO thin films was 8 nm.

In order to take advantage of the biosensing capability of the rGO thin films in their lateral direction, in-line EIS measurements were carried out (Fig. 2a). The impedance signals were collected along the rGO thin film to address the bio-recognition process. Already at small frequencies of 1 Hz the responses were stable and showed a reliable biosensor readout. Mathematically, the impedance Z is expressed either in its polar form $Z = |Z|e^{j\varphi}$ or the Euler's form $Z = Z_1 + jZ_2$ which are noted as Bode plot and Nyquist plot, respectively. In our study, the Bode plot was used to analyze the biosensing performance of the rGO IDEs. The equivalent circuit as shown in Fig.2c can be used to simulate the experimentally obtained Bode plots. The reason to build up such an equivalent circuit are as following: For the current flow inside the quilted layer, the rGO thin film can be treated as a resistor R_{rGO} in parallel to a capacitor C_{rGO}. The capacitance behavior of the rGO thin film was also proven by C-V measurements in dry status (supporting information **S1**). In these measurements, the rGO thin film clearly formed Ohmic contacts with the IDEs, but were acting as capacitors under AC stimulation. For the current flow through the buffer solution on top of the IDEs, the equivalent electrical circuit of two EDLs composed of a resistor and a constant phase element (CPE, is symbolized by Q,

$Z = 1/(j\omega Q^n)$) are both in series with the solution resistance R_{Sol}. To model this, we used a CPE instead of an ideal capacitor. This choice was proven by carrying out measurements with the same rGO IDEs devices in the configuration of in-line, and classical out-of-line EIS (supporting information **S2**). The out-of-line EIS measurements were carried out in 10 mM PB solution as well, where both arms of IDEs structures were acting as one working electrode (WE), an additional Pt wire and the Ag/AgCl electrode served as counter electrode (CE) and reference electrode (RE), respectively (supporting information, **Fig. S2**). For these measurements, we used an input V_{in} (t) of 10 mV amplitude as well within a frequency range from 1Hz to 100kHz and a DC bias voltage of 50 mV, similar to the in-line experiments. From the measurements, we can extract the equivalent circuit elements of the EDLs at the interface of the rGO thin films and the buffer solution. As demonstrated by the out-of-line EIS experiments, the EDL built on rGO surface is not an ideal capacitor, because the slope in the Nyquist plots is not 45° (supporting material, **Fig. S2c**). In this case, a constant phase element (CPE) was used instead. Based on this equivalent circuit model, the values of the electronic elements of the circuit can be extracted from the simulation: $R_{rGO} = 900\ k\Omega$, $C_{rGO} = 1.37\ nF$, $R_{sol} = 2830\Omega$, $R_{int1} = 9.84 \times 10^{-7}\Omega$, $Q_1 = 1.2 \times 10^{-6}$, $n_1 = 0.7$. $R_{int2} = 2.196 \times 10^{7}\Omega$, $Q_2 = 1.2 \times 10^{-6}$, $n_2 = 0.7$.

To evaluate the biosensing capability, rGO IDEs devices were tested in in-line EIS configuration to detect PSA. The biosensors were prepared with anti-PSA aptamers as receptor biomolecules using standard EDC/NHS linking chemistry and ethanolamine as blocking agent to suppress unspecific binding (Fig. 3a). An aptamer usually consists of a short single-stranded DNA sequence. It is of small size and high stability, providing a high affinity towards their targets very similar to antibodies with a very sensitive binding of small,

organic compounds, large proteins and even whole cells. The structure of the anti-PSA aptamer used in our study is folded with a hairpin loop, because two regions of the stand are complementary and form local Watson-Crick base pairs (Fig. 3B). The aptamer sizes in this configuration are approximately 3-5 nm. The molecular weight of PSA is 33 kDa and its diameter is approximately 4.5 nm. The PSA detection was done in 10 mM PB solution with an ionic strength 162 mM and corresponding Debye length of 0.76 nm. The Debye length depends on the solvent permittivity $\varepsilon_s = \varepsilon_0 \varepsilon_r$, number concentrations of the solute ions $n_{i\infty}$ (/m^3) and valence of the solute ions Z_i by following the equation: $\kappa^{-1} = \sqrt{\frac{\varepsilon_s k_B T}{\sum_i n_{i\infty} {Z_i}^2 e^2}}$, in which the vacuum permittivity $\varepsilon_0 = 8.854 \times 10^{-12}\, F \cdot m^{-1}$, relative permittivity of water $\varepsilon_r = 78$, Boltzmann constant $k_B = 1.38 \times 10^{-23}\, J \cdot K^{-1}$, room temperature $\mathrm{T} = 300\, K$, the charge of an electron $\mathrm{e} = 1.602 \times 10^{-19}$ C, the ion number $n_{i\infty}$= molar concentration × N_A, Avogadro constant $N_A = 6.02 \times 10^{-23} mol^{-1}$. This measurement condition is very similar to the case in physiological solution, which typically has an ionic strength of approximately 150 mM and its corresponding Debye length is 0.8 nm. The descriptive schematic of the EDL with biomolecules in our study are given in Fig. 3b. In this condition, a typical field-effect based semiconductor biosensor will hardly show any sensing due to the Debye-screening of charges. The bound PSA targets locate outside the EDL, so their charges should not be able to modulate the surface potential of the transducer layer.

However, in our experiments the rGO IDE based in-line EIS biosensors exhibited a very good sensing performance beyond this Debye-screening limit. The Bode plots (Fig.4a) obtained from PSA dose-response experiments show sensing capability at a low frequency range of 1-10 Hz and in the impedance phase around 1 kHz. The bonded PSA leads to

increases of impedance amplitudes at these frequencies (Fig.4b). The biosensor without aptamer receptor molecules were measured in 10 mM PB solution for 3 times exchange of the test solution and 1 times exchange of the cable. The baseline of the experiments was calculated from these four measurements. HSA was used as highly concentrated, non-specific control experiment. After 1 µM HSA incubation, three channels were measured two times to obtain the non-specific control signal. The specific signals corresponding to the PSA binding can be clearly distinguished from the non-specific signal (red color) of 1 µM HSA. The limit of detection was about 33 pM. In Fig. 4c the clinically relevant concentration range is marked (4-10ng/ml corresponding to 115-290pM). It can be seen that our sensor platform perfectly matches this range with highest signal resolution there.

To reveal the sensing mechanism of the bio-recognition capability beyond the Debye-screening limitation at low frequencie,s the dose-response of rGO-IDEs aptasensor to detect PSA were also measured by dual I-V sweeps. The obtained results (supporting information **S3**) show that the PSA binding also leads to an increase of the rGO thin film resistance. This coincides with the results from the PSA dose-response experiments with the in-line EIS configuration. It is obvious from these findings that the rGO thin films can respond to binding of PSA biomolecules. Eventually this binding leads to a disturbance of the EDL on top of the rGO material. This would affect the rGO layer in terms of its ‘gate dielectrics’, which is this EDL rather than the direct detection of the biomolecule charges. The tendency of the observed resistance increases can be explained by the bipolar transport properties of the rGO thin films (Fig. S3b-3c). PSA is negatively charged. Therefore, the surface potential change on the rGO thin film is in total negative. In an ideal case, the carrier type affected by this should be the bipolar left

arm of the characteristics (holes as dominant carrier). Because the Dirac point was shifted to the left as well, the responding carriers are at the bipolar right arm (electrons as dominant carriers). The more PSA molecules bind, the larger amount of negative gate voltage is applied to the rGO thin film. Therefore, the conductivity of the rGO channel decreases and its resistance increases. This could explain the results obtained in our in-line EIS and the dual I-V sweep experiments for PSA detection.

5. Conclusions

The ultra-thin rGO films structured on top of micro sized IDE sensors were utilized as transducer layer for an in-line, electrochemical impedance spectroscopy aptasensor platform to detect PSA. The dose-response measurements were carried out in 10 mM buffer solution, which has an ionic strength of 162 mM and hence a Debye length onlky 0.76 nm. This test solution is very close to typical physiological solutions such as blood serum. The biosensor signals were extracted from impedance amplitudes in Bode plots at low frequencies (1-10 Hz). The sensing range of the PSA biosensors covered a wide range from 33 pM to 330 nM showing increasing impedance amplitudes. We demonstrated that our rGO thin films preserve a bipolar transport property similar to graphene with the clear advantage to be integrated into a standard process flow as spin-coating layer. The binding of PSA biomolecules increased the rGO channel impedance amplitudes at low frequency levels i.e. resistances. This tendency was confirmed by DC I-V sweeps which showed similar changes. The established biosensor platform can detect PSA fully covering its clinically relevant range (4-10 ng/ml) in physiological buffer concentrations. We are fully convinced that our work lightens up the application direction to use rGO thin-films as nanometer thick transducer layers in biosensor platforms to directly detect various biomarkers in physiological matrices.

Supporting Information

The supporting information file contains characterizations of rGO thin films in dry conditions and in a classical EIS configuration. In addition the PSA detection results recorded in DC I-V sweeps are presented there.

Acknowledgments

This work was funded by the European Commission Program through the Marie Curie Initial Training Network PROSENSE (grant no. 317420, 2012-2016, www.prosense-itn.eu). Vivek Pachauri thanks the Euroimmun AG and the Stiftung Rheinland-Pfalz für Innovation (grant no. 1082) for funding of his position. The authors thank Detlev Cassel for his support in device fabrication and Rainer Lilischkis (both University of Applied Sciences Kaiserslautern, Germany) for his support with SEM imaging.

6. References

Antenor, J.A. V., Roehl, K.A., Eggener, S.E., Kundu, S.D., Han, M., Catalona, W.J., 2005. Preoperative PSA and progression-free survival after radical prostatectomy for Stage T1c disease. Urology 66, 156–160. https://doi.org/10.1016/j.urology.2005.01.008

Baade, P.D., Youlden, D.R., Krnjacki, L.J., 2009. International epidemiology of prostate cancer: Geographical distribution and secular trends. Mol. Nutr. Food Res. https://doi.org/10.1002/mnfr.200700511

Bagri, A., Mattevi, C., Acik, M., Chabal, Y.J., Chhowalla, M., Shenoy, V.B., 2010. Structural evolution during the reduction of chemically derived graphene oxide. Nat. Chem. 2, 581–587. https://doi.org/10.1038/nchem.686

Baringhaus, J., Ruan, M., Edler, F., Tejeda, A., Sicot, M., Taleb-Ibrahimi, A., Li, A.-P., Jiang, Z., Conrad, E.H., Berger, C., Tegenkamp, C., de Heer, W.A., 2014. Exceptional ballistic transport in epitaxial graphene nanoribbons. Nature 506, 349–354.

Barsoukov, E., Macdonald, J.R., 2005. Impedance Spectroscopy: Theory, Experiment, and Applications, 2nd Edition. WILEY. https://doi.org/10.1002/0471716243

Bart, M., Stigter, E.C.A., Stapert, H.R., De Jong, G.J., Van Bennekom, W.P., 2005. On the response of a label-free interferon-γ immunosensor utilizing electrochemical impedance spectroscopy. Biosens. Bioelectron. 21, 49–59. https://doi.org/10.1016/j.bios.2004.10.009

Berdat, D., Marin, A., Herrera, F., Gijs, M.A.M., 2006. DNA biosensor using fluorescence microscopy and impedance spectroscopy. Sensors Actuators, B Chem. 118, 53–59. https://doi.org/10.1016/j.snb.2006.04.064

Berdat, D., Rodríguez, A.C.M., Herrera, F., Gijs, M.A.M., 2008. Label-free detection of DNA with interdigitated micro-electrodes in a fluidic cell. Lab Chip 8, 302–308. https://doi.org/10.1039/B712609C

Bonanni, A., Ambrosi, A., Pumera, M., 2012a. Nucleic acid functionalized graphene for biosensing. Chem. - A Eur. J. 18, 1668–1673. https://doi.org/10.1002/chem.201102850

Bonanni, A., Loo, A.H., Pumera, M., 2012b. Graphene for impedimetric biosensing. TrAC - Trends Anal. Chem. 37, 12–21. https://doi.org/10.1016/j.trac.2012.02.011

Castro Neto, A.H., Guinea, F., Peres, N.M.R.M.R., Novoselov, K.S.S., Geim, A.K.K., 2009. The electronic properties of graphene. Rev. Mod. Phys. 81, 109–162. https://doi.org/10.1103/RevModPhys.81.109

De, S., Coleman, J.N., 2010. Are There Fundamental Limitations on the Sheet Resistance and Transmittance of Thin Graphene Films? ACS Nano 4, 2713–2720. https://doi.org/10.1021/nn100343f

Dreyer, D.R., Park, S., Bielawski, C.W., Ruoff, R.S., 2010. The chemistry of graphene oxide. Chem. Soc. Rev. 39, 228–240. https://doi.org/10.1039/B917103G

Eda, G., Chhowalla, M., 2010. Chemically derived graphene oxide: towards large-area thin-film electronics and optoelectronics. Adv. Mater. 22, 2392–2415.

Formisano, N., Jolly, P., Bhalla, N., Cromhout, M., Flanagan, S.P., Fogel, R., Limson, J.L., Estrela, P., 2015. Optimisation of an electrochemical impedance spectroscopy aptasensor by exploiting quartz crystal microbalance with dissipation signals. Sensors Actuators B Chem. 220, 369–375. https://doi.org/10.1016/j.snb.2015.05.049

Geim, A.K., Novoselov, K.S., 2007. The rise of graphene. Nat. Mater. 6, 183–191.

Gómez-Navarro, C. et al., 2007. Electronic transport properties of individual chemically reduced graphene oxide sheets. Nano Lett. 7, 3499–3503.

Huang, P.Y., Ruiz-Vargas, C.S., van der Zande, A.M., Whitney, W.S., Levendorf, M.P., Kevek, J.W., Garg, S., Alden, J.S., Hustedt, C.J., Zhu, Y., Park, J., McEuen, P.L., Muller, D.A., 2011. Grains and grain boundaries in single-layer graphene atomic patchwork quilts. Nature 469, 389–392.

Igreja, R., Dias, C.J., 2004. Analytical evaluation of the interdigital electrodes capacitance for a multi-layered structure. Sensors Actuators A Phys. 112, 291–301.

Jolly, P., Formisano, N., Tkáč, J., Kasák, P., Frost, C.G., Estrela, P., 2015. Label-free impedimetric aptasensor with antifouling surface chemistry: A prostate specific antigen case study. Sensors Actuators, B Chem. 209, 306–312. https://doi.org/10.1016/j.snb.2014.11.083

Kahng, Y.H., Lee, S., Park, W., Jo, G., Choe, M., Lee, J.-H., Yu, H., Lee, T., Lee, K., 2012. Thermal stability of multilayer graphene films synthesized by chemical vapor deposition and stained by metallic impurities. Nanotechnology 23, 75702. https://doi.org/10.1088/0957-4484/23/7/075702

Lanche, R., Pachauri, V., Koppenhöfer, D., Wagner, P., Ingebrandt, S., 2014. Reduced graphene oxide-based sensing platform for electric cell-substrate impedance sensing. Phys. Status Solidi Appl. Mater. Sci. 211, 1404–1409. https://doi.org/10.1002/pssa.201330522

Liang, X., Sperling, B.A., Calizo, I., Cheng, G., Hacker, C.A., Zhang, Q., Obeng, Y., Yan, K., Peng, H., Li, Q., Zhu, X., Yuan, H., Walker, A.R.H., Liu, Z., Peng, L., Richter,

C.A., 2011. Toward Clean and Crackless Transfer of Graphene. ACS Nano 5, 9144–9153.

Lisdat, F., Schafer, D., 2008. The use of electrochemical impedance spectroscopy for biosensing. Anal. Bioanal. Chem. 391, 1555–1567. https://doi.org/10.1007/s00216-008-1970-7

Lu, X., Munief, W.-M., Heib, F., Schmitt, M., Britz, A., Grandthyl, S., Müller, F., Neurohr, J.-U., Jacobs, K., Benia, H.M., Lanche, R., Pachauri, V., Hempelmann, R., Ingebrandt, S., 2018. Front-End-of-Line Integration of Graphene Oxide for Graphene-Based Electrical Platforms. Adv. Mater. Technol. 1700318, 1700318. https://doi.org/10.1002/admt.201700318

Macdonald, J.R., 2005. Impedance spectroscopy: Models, data fitting, and analysis. Solid State Ionics 176, 1961–1969. https://doi.org/http://dx.doi.org/10.1016/j.ssi.2004.05.035

Macdonald, J.R., 1990. Impedance spectroscopy: old problems and new developments. Electrochim. Acta 35, 1483–1492. https://doi.org/http://dx.doi.org/10.1016/0013-4686(90)80002-6

Novoselov, K.S., Fal'ko, V.I., Colombo, L., Gellert, P.R., Schwab, M.G., Kim, K., 2012. A roadmap for graphene. Nature 490, 192–200. https://doi.org/10.1038/nature11458

Novoselov, K.S., Geim, A.K., Morozov, S. V, Jiang, D., Zhang, Y., Dubonos, S. V, Grigorieva, I. V, Firsov, A.A., 2004. Electric Field Effect in Atomically Thin Carbon Films. Science 306, 666–669. https://doi.org/DOI: 10.1126/science.1102896

Orazem, M.E., Tribollet, B., 2011. Electrochemical Impedance Spectroscopy. WILEY . https://doi.org/10.1002/9780470381588

Pei, S., Cheng, H.-M.M., 2012. The reduction of graphene oxide. Carbon N. Y. 50, 3210–3228. https://doi.org/http://dx.doi.org/10.1016/j.carbon.2011.11.010

Schmitt, M., 2014. Analysis of silanes and of siloxanes formation by Raman spectroscopy †. RSC Adv. 4, 1907–1917. https://doi.org/10.1039/C3RA45306E

Schmitt, M., Hempelmann, R., Ingebrandt, S., Munief, W.-M., Gross, K., Grub, J., Heib, F., 2015. Statistical approach for contact angle determination on inclining surfaces: "slow-moving" analyses of non-axisymmetric drops on a flat silanized silicon wafer. J. Adhes. Sci. Technol. 29, 1796–1806. https://doi.org/10.1080/01694243.2014.976000

Suk, J.W., Kitt, A., Magnuson, C.W., Hao, Y., Ahmed, S., An, J., Swan, A.K., Goldberg, B.B., Ruoff, R.S., 2011. Transfer of CVD-Grown Monolayer Graphene onto Arbitrary Substrates. ACS Nano 5, 6916–6924.

Yang, L., Li, Y., Erf, G.F., 2004. Interdigitated Array Microelectrode-Based Electrochemical Impedance Immunosensor for Detection of Escherichia coli O157:H7. Anal. Chem. 76, 1107–1113. https://doi.org/10.1021/ac0352575

Zaretsky, M.C., Mouayad, L., Melcher, J.R., 1988. Continuum properties from interdigital electrode dielectrometry. Electr. Insul. IEEE Trans. 23, 897–917.

Figures

Fig. 1. Characterizations of rGO thin-films: (A) Scanning electron microscopy image of an rGO thin-film patterned on top of interdigitated gold microelectrodes (IDEs). (B) Atomic force microscopic image of a GO thin-film at the edge of a structured pattern. Step size shows a thickness of 8 nm with a smooth GO surface.

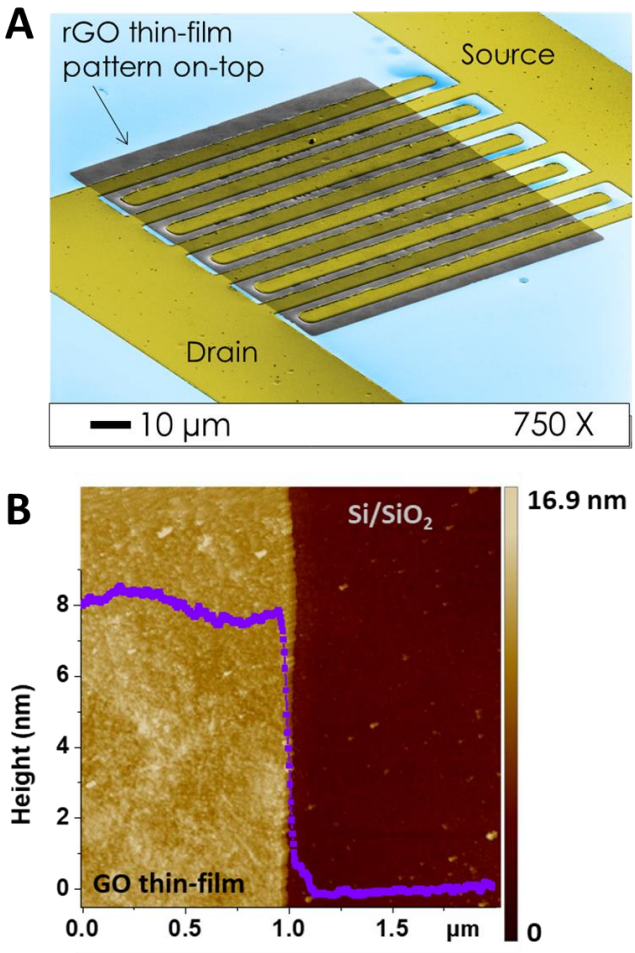

Fig. 2. Electronic characterization of the rGO thin-film based in-line EIS: (A) Schematics of an rGO thin-film in EIS configuration, where the two arms of the IDE structures and an electrochemical Ag/AgCl electrode serve as working electrode (WE), counter electrode (CE) and reference electrode (RE), respectively. (B) Experimental and simulated Bode plots of in-line impedimetric spectroscopy with rGO thin films as transducer layers in 10 mM PB solution. (C) Equivalent circuits of rGO thin-film based in-line impedimetric spectroscopy in aqueous solution. $R_{int1(2)}$ and $Q_{int1(2)}$ are the resistance and capacitance of the electrical double layers that build up on the interface of the electrodes and the liquid. R_{sol} is the resistance of the electrolyte solution. R_{rGO} and C_{rGO} are the resistance and the capacitance of the rGO thin film, respectively. Value of the equivalent circuit elements are listed in the table.

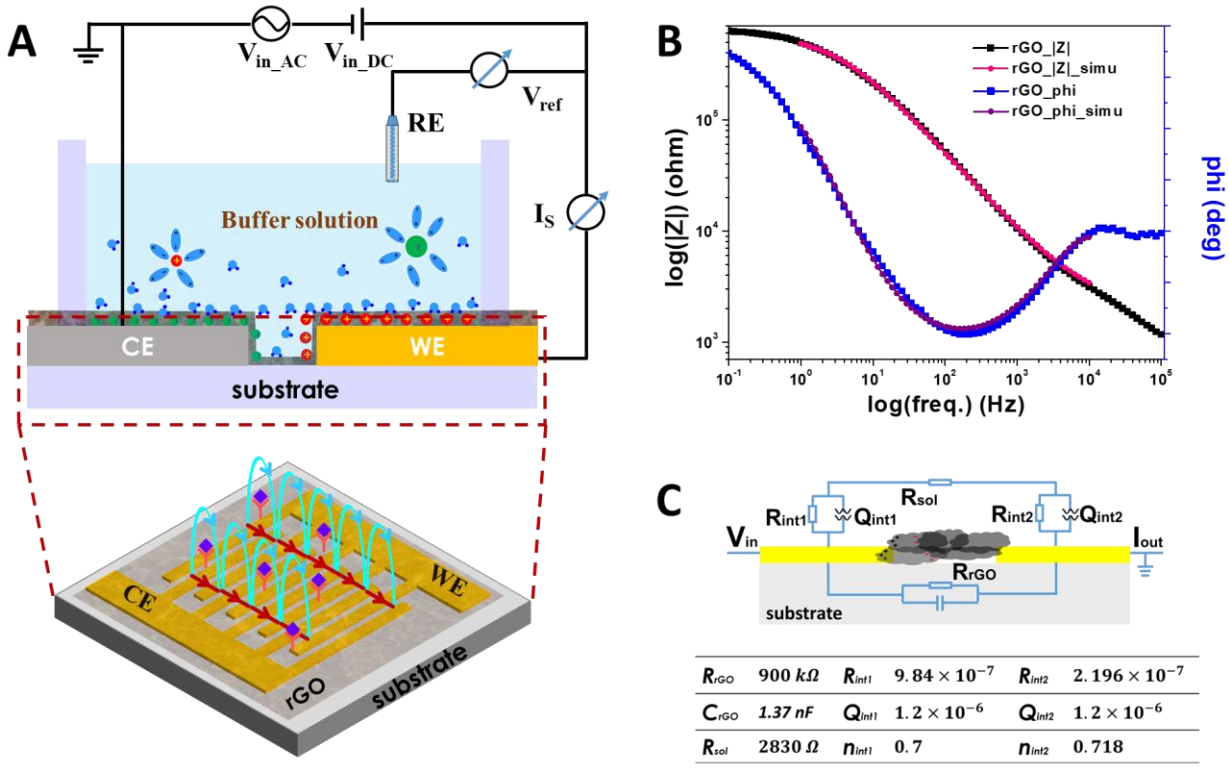

R_{rGO}	900 kΩ	R_{int1}	9.84×10^{-7}	R_{int2}	2.196×10^{-7}
C_{rGO}	1.37 nF	Q_{int1}	1.2×10^{-6}	Q_{int2}	1.2×10^{-6}
R_{sol}	2830 Ω	n_{int1}	0.7	n_{int2}	0.718

Fig. 3. Descriptive schematics of an rGO IDE EIS experiment to detect PSA: (A) Preparation flow of aptasensors: The -COOH groups on the surface of rGO thin film were activated by EDC/NHS chemistry, so that the amino-terminated receptor biomolecules can be immobilized. Afterwards, the surface was saturated by ethanolamine to suppress non-specific binding. In the following, PSA was detected. (B) Descriptive schematics of an rGO IDE biosensor with aptamer receptor biomolecules, which locates within the Debye length (0.76 nm) on the rGO transducer layer.

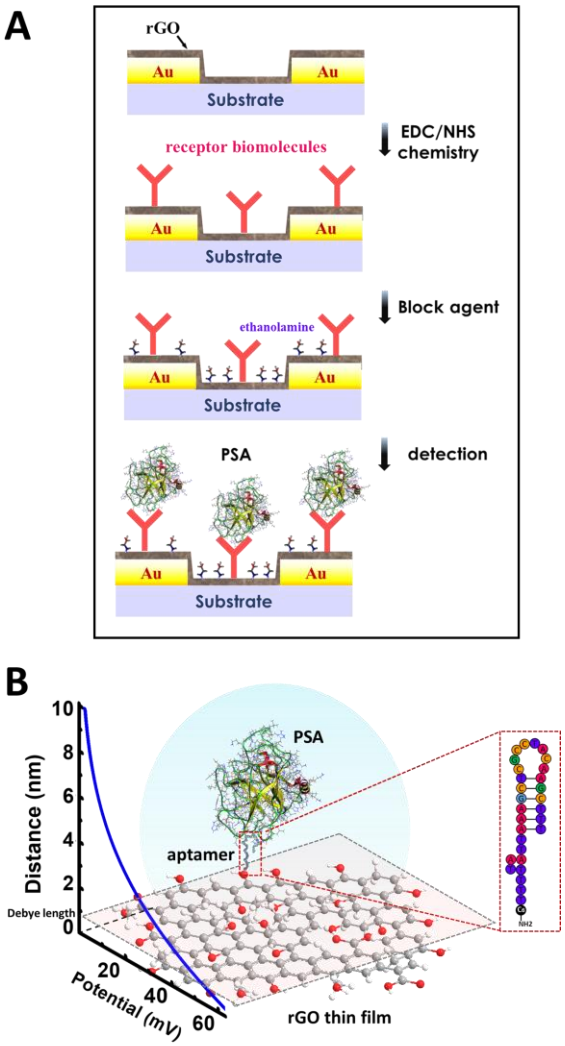

Fig. 4. Dose-response experiment to extract a calibration curve for PSA detection: (A) Bode plot of the PSA dose-response experiments. (B) The close-up shows the impedance amplitudes at low frequencies (1-5 Hz). (C) Amplitude calibration curve of the PSA dose-response experiments by rGO-based, in-line EIS with aptamers as receptor molecules in physiological buffer solution. 1 µM human serum antigens (HSA) was used as a non-specific control (red data point).

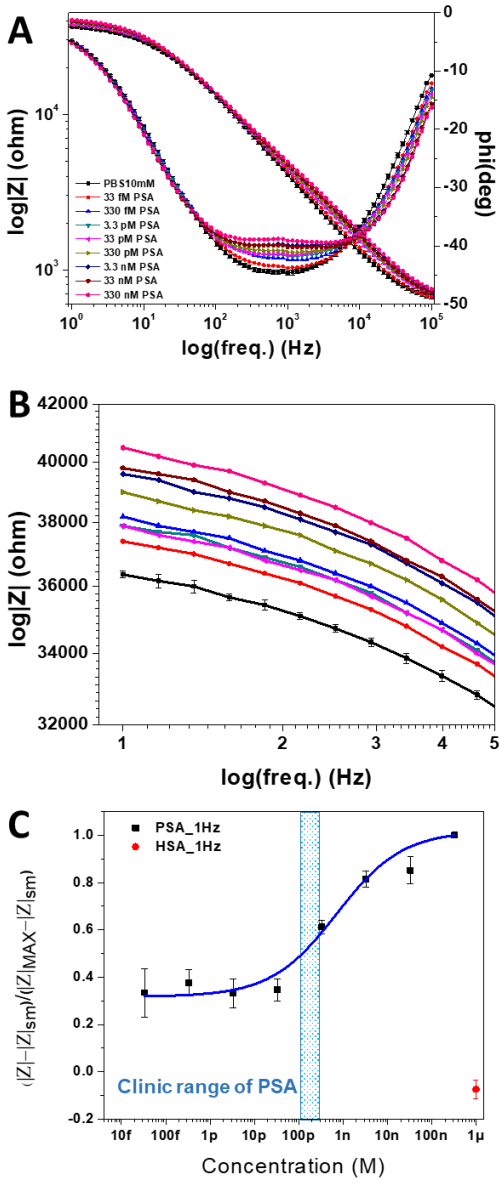

Highlights:

1. We developed a process to fabricate highly reproducible biosensors based on interdigitated electrode (IDE) structures. These structures we bridged with reduced graphene oxide (rGO) thin films.
2. Reduced graphene oxide thin films exhibit a bipolar carrier transport characteristics similar to pristine graphene. We read out the rGO based IDEs in an in-line electrochemical impedance spectroscopy configuration.
3. Sensors were functionalized with short aptamers, which are highly specific to prostate specific antigens (PSA). At low frequency (1-10 Hz) sensors showed robust response towards different concentrations of PSA. A control experiment did not show a response demonstrating the highly specific PSA detection.
4. Detection was possible in a physiological buffer concentration with a Debye-length similar to human serum. Therefore, this sensor scheme can overcome the typical Debye-screening limitation of charges in liquid environments.
5. The limit of detection and the high resolution of the readout is fully covering the clinically relevant concentration range for biomedical application of this assay.

Highlights:

1. We developed a process to fabricate highly reproducible biosensors based on interdigitated electrode (IDE) structures. These structures we bridged with reduced graphene oxide (rGO) thin films.
2. Reduced graphene oxide thin films exhibit a bipolar carrier transport characteristics similar to pristine graphene. We read out the rGO based IDEs in an in-line electrochemical impedance spectroscopy configuration.
3. Sensors were functionalized with short aptamers, which are highly specific to prostate specific antigens (PSA). At low frequency (1-10 Hz) sensors showed robust response towards different concentrations of PSA. A control experiment did not show a response demonstrating the highly specific PSA detection.
4. Detection was possible in a physiological buffer concentration with a Debye-length similar to human serum. Therefore, this sensor scheme can overcome the typical Debye-screening limitation of charges in liquid environments.
5. The limit of detection and the high resolution of the readout is fully covering the clinically relevant concentration range for biomedical application of this assay.

Cover Letter

Institut für Werkstoffe der Elektrotechnik 1

RWTH AACHEN UNIVERSITY

Univ.-Prof. Dr. rer. nat.
Sven Ingebrandt
Professor for Micro- and Nanosystems

Sommerfeldstr. 24
52074 Aachen
GERMANY
Phone: +49 241 80-27810/11
Fax: +49 241 80-22392
Room: 24C314

ingebrandt@iwe1.rwth-aachen.de

My symbol: SI
01.07.2018

IWE1 | Sommerfeldstraße 24, 52074 Aachen, Germany 612510

Biosensors and Bioelectronics
Editorial office
Dr. Alice Tang Turner

Submission of our manuscript to the Biosensors 2018 special issue of Biosensors and Bioelectronics

Dear Dr. Tang,

We submit our manuscript '***Reduced Graphene-Oxide Transducers for Biosensing Applications Beyond the Debye-Screening Limit***' to Biosensors and Bioelectronics and we sincerely hope it can be included into the special issue 'Biosensors 2018' of this journal. The results were presented by me personally at this conference in Miami on behalf of the first author Xiaoling Lu, who unfortunately did not get her travel visa to USA in time.

Poster number of our presentation was: P1.165

Our manuscript summarizes the results of a cooperative work in the framework of the EU project PROSENSE (www.prosense-itn.eu), where Ms. Lu was one of the 'early stage researcher' fellows towards her PhD. We hope that you find our work worth to be published in Biosensors and Bioelectronics.

Sincerely on behalf of all authors,

Prof. Dr. Sven Ingebrandt
RWTH Aachen University

Supplementary Material

Click here to download Supplementary Material: PSA impedance rGO biosensor B+B_Supporting Information_FINAL.docx